Dynamics of GaAs/AlGaAs microdisk lasers

K. J. Luo, J. Y. Xu, and H. Cao[a)]
Department of Physics and Astronomy, Northwestern University, Evanston, Illinois 60208-3112

Y. Ma, S. H. Chang, and S. T. Ho
Department of Electrical and Computer Engineering, Northwestern University, Evanston, Illinois 60208-3118

G. S. Solomon
Department of Electrical Engineering, Stanford University, Stanford, California 94305

(Received 8 June 2000; accepted for publication 17 August 2000)

Dynamic response of a GaAs/AlGaAs microdisk laser has been experimentally investigated using femtosecond optical pumping. Below the lasing threshold, the delay time of the emission pulse from the microdisk hardly changes with the pump power. Above the lasing threshold, the delay time is shortened dramatically, and it decreases with increasing the pump power. The theoretical simulation based on the rate equations reproduces the experimental observation after the effect of carrier diffusion is taken into account. The simulation result illustrates that the speed of a microdisk laser is limited mainly by the carrier diffusion in the disk plane.
[S0003-6951(00)04041-9]

Semiconductor microdisk lasers have attracted much attention in the past decade due to their potential applications in photonic integrated circuits.[1] The advantages of microdisk lasers are small cavity volume and high quality factor Q for whispering gallery modes. These two factors result in large spontaneous emission factor β, which can be of the order of 0.1. Furthermore, ultralow lasing threshold has been achieved in both optically[2–6] and electrically[7–10] pumped microdisk lasers. The low power consumption makes the microdisk laser a promising candidate for the light emitter in a large-scale photonic circuit. However, for many laser applications, not only low lasing threshold but also high speed is desired. For example, how fast a laser can be modulated is very important for the applications in optical communication. Up to now, almost all the research work on microdisk lasers are focused on the steady-state properties. The dynamic behavior of the microdisk laser is rarely studied. In this letter, we will investigate the dynamic response of a GaAs/AlGaAs microdisk laser using femtosecond optical pumping. It is found that the turn-on time of a 5-μm-microdisk laser is less than 100 ps. Our theoretical simulation based on rate equations illustrates that the speed of a microdisk laser is limited mainly by the carrier diffusion in the disk plane.

The sample investigated in our experiments consists of a 300-nm-GaAs buffer layer, a 500-nm-$Al_{0.7}Ga_{0.3}As$ layer, three 20-nm-GaAs quantum wells sandwiched between 30-nm-$Al_{0.7}Ga_{0.3}As$ barriers, and 20-nm-GaAs cap layer. The sample is grown by molecular-beam-epitaxy on a (100) semi-insulating GaAs substrate. The photoluminescence (PL) spectrum of the unprocessed wafer is centered around 820 nm with a full width at half maximum (FWHM) of 5 nm at 77 K.

a)Electronic mail: h-cao@nwu.edu

The microdisks are fabricated by optical lithography and two steps of wet etch.[11] The diameter of the disks is 5 μm. Each disk is supported by a 500-nm-long $Al_{0.7}Ga_{0.3}As$ pedestal. The microdisk is optically excited by 200 fs pulses from a mode-locked Ti:sapphire laser with the repetition rate of 76 MHz. The excitation wavelength is fixed at 780 nm (1.59 eV). The pump beam is focused onto a single microdisk by a microscope objective. The sample is mounted in a liquid helium cryostat, and all the experimental data are recorded at 4.2 K. The pump beam is incident normally onto the microdisk through the front window of the cryostat. To collect efficiently the far-field emission from the whispering gallery modes, a lens is placed next to the side window of the cryostat to collect the emission from the side of the microdisk. A bandpass filter is used to attenuate the scattered pump light. The emission from the microdisk is measured simultaneously by a synchroscan streak camera and a 0.5 m spectrometer with a cooled CCD array detector. The temporal resolution of the streak camera is 8 ps. The spectral resolution of the spectrometer is 0.17 nm.

The time-resolved traces and time-integrated spectra of microdisk emission at different pump powers are shown in Figs. 1(a) and 1(b), respectively. The first peak in the time trace shown in Fig. 1(a) corresponds to the scattered pump pulse, acting as the zero of the time marker. After a certain delay, the emission from the microdisk reaches its maximum and then decays. When the incident pump power is less than 35 μW, the emission signal is quite weak, and the time it takes to reach the maximum hardly changes as the pump power increases. However, when the pump power exceeds 35 μW, a short emission pulse appears around 200 ps. The time between its maximum and the pump pulse decreases significantly with increasing the pump power. At the pump powers of 40 and 60 μW, relaxation oscillation is clearly observed in the time-resolved traces. On the other hand, in the emission spectra shown in Fig. 1(b), the magnitude of the peak at 818 nm increases over one order of magnitude when

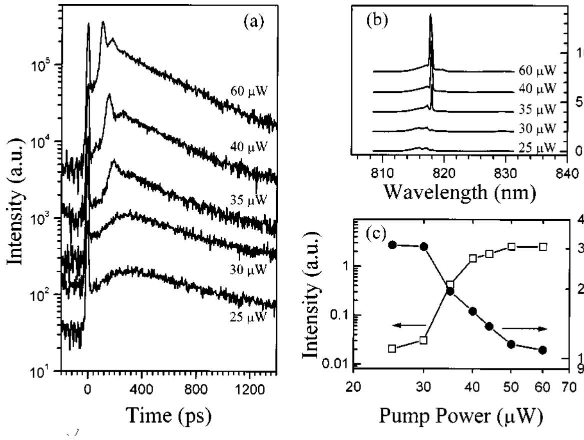

FIG. 1. (a) Experimentally observed temporal evolution of microdisk emission. (b) Time-integrated emission spectra. The incident pump powers are marked next to the curves, which are shifted vertically for clarity. (c) The integrated emission intensity and the delay time as a function of the incident pump power.

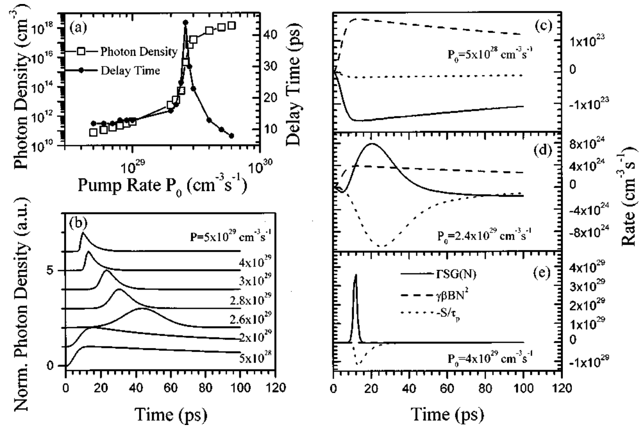

FIG. 2. Calculated results when the pump pulse width is 10 ps. (a) The maximum photon density and the delay time vs the pump rate. (b) The temporal evolution of the photon density at several pump rates as indicated. (c)–(e) The time-resolved traces of $\Gamma SG(N)$ (solid line), $\gamma\beta BN^2$ (dashed line), and $-S/\tau_p$ (dotted line) at several pump rates as indicated.

the pump power exceeds 35 μW, and the FWHM of the peak narrows to 0.15 nm. These data indicate lasing oscillation at 818 nm. Figure 1(c) plots the spectrally integrated emission intensity and the delay time (i.e., the time between the pump pulse and the maximum of the emission pulse) as a function of the incident pump power. It can be seen clearly that the delay time experiences a sudden decrease near the lasing threshold. We believe this phenomenon is caused by the fast stimulated emission, which becomes dominant over the slow spontaneous emission above the lasing threshold. In the following, we will simulate the dynamics of the microdisk laser using the rate equation model.

The rate equations for a microcavity laser can be written as:[1,12]

$$\frac{dN}{dt}=-\Gamma SG(N)-\left(\frac{A_a}{V_a}v_sN+\gamma BN^2\right)+P_p(t), \tag{1}$$

$$\frac{dS}{dt}=\Gamma SG(N)+\gamma\beta BN^2-\frac{S}{\tau_p}, \tag{2}$$

where N denotes the carrier density in the active region, S the photon density in the laser mode, Γ the optical confinement factor, $G(N)$ the gain coefficient. A_a and V_a are the surface area and volume of the active region, respectively, v_s the surface recombination velocity, B the spontaneous emission coefficient in a bulk semiconductor material, γ the enhancement factor of the spontaneous emission rate in a microcavity, $P_p(t)$ the carrier injection rate, β the spontaneous emission factor which is defined as the ratio of spontaneous emission rate for one laser mode to all the modes, and τ_p the photon lifetime. The first term on the right-hand side of Eq. (1) accounts for stimulated emission rate, the second term for surface recombination rate and spontaneous emission rate, and the third term for external pump rate. The pump pulse is assumed to be Gaussian, i.e., $P_p(t)=P_0e^{-(2t/w\sqrt{\ln 2})^2}$, where w is the FWHM of the pulse. We calculate $\Gamma=0.45$, $\gamma=1.0$, $\beta=0.01$ for the lowest order TE mode in a 5 μm disk. For GaAs quantum wells, $v_s\simeq 2.5\times 10^5$ cm/s and $B\simeq 2.5\times 10^{-10}\,\mathrm{cm}^3/\mathrm{s}$.[1] The gain coefficient $G(N)=G_0(N-N_0)$, where N_0 represents the carrier density at the transparency point.[13] In our case, $G_0\simeq 5\times 10^{-6}\,\mathrm{cm}^3/\mathrm{s}$, $N_0\simeq 1.16\times 10^{18}\,\mathrm{cm}^{-3}$.[1] From the spectral linewidth of the whispering gallery mode near the lasing threshold (i.e., the transparency point), we estimate the cavity quality factor $Q\equiv\lambda_0/\Delta\lambda=5450$, corresponding to a photon lifetime (τ_p) of 5 ps. Taking into account the carrier relaxation, we assume the pulse of carrier injection $P_p(t)$ has a FWHM of 10 ps.[14] Using the above parameters, we solve the rate equations [Eqs. (1) and (2)] numerically for $N(t)$ and $S(t)$. Figure 2(a) plots the calculated delay time and the maximum photon density at different pump rates. The temporal evolution of the photon density $S(t)$ is shown in Fig. 2(b). In Fig. 2(a), the photon density increases over 2 orders of magnitude and the delay time jumps down when P_0 is beyond the lasing threshold ($2.6\times 10^{29}\,\mathrm{cm}^{-3}\,\mathrm{s}^{-1}$). In addition, the delay time increases significantly with P_0 before the threshold is reached. In order to understand this behavior, we plot each of the three terms on the right-hand side of Eq. (2) as a function of time at different pump rate P_0 in Figs. 2(c)–2(e). When P_0 is much lower than the threshold, the first term $\Gamma SG(N)$ is always negative, corresponding to optical absorption. Thus the initial rise of the photon density is attributed to the second term which represents the spontaneous emission. Since the spontaneous emission rate does not change much with P_0, the delay time is nearly constant. However, when P_0 is very close to (but less than) the threshold, $\Gamma SG(N)$ becomes positive over a period of time, and then negative, as shown in Fig. 2(d). When $\Gamma SG(N)$ is positive, the stimulated emission also contributes to the increase of the photon density. Thus, the time it takes to reach the maximum photon density increases. Subsequently, $\Gamma SG(N)$ becomes negative due to the depletion of the excited carriers, and the optical absorption causes a decrease of the photon density. Therefore, the time evolution of the photon density is determined by both spontaneous and stimulated emission in this case. After P_0 reaches the threshold, the stimulated emission dominates [see Fig. 2(e)]. The photon density increases rapidly in time, leading to a sudden drop of the delay time. As the pump rate increases further, the stimulated emission rate increases and the delay time decreases.

Although the simulated results at P_0 above or well below the lasing threshold agree qualitatively with the experi-

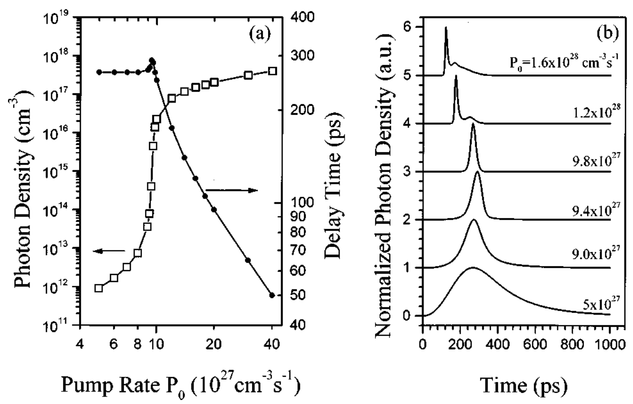

FIG. 3. Calculated results when the pump pulse width is 400 ps. (a) The maximum photon density and delay time as a function of the pump rate. (b) The temporal evolution of the photon density at several pump rates as indicated.

mental data, the calculated delay time is much less than the experimental value, and the increase of the delay time as P_0 approaches the lasing threshold is not observed experimentally. Moreover, the relaxation oscillation does not appear in the calculated time trace of $S(t)$ above the threshold. This is because the pump pulse is so short that the photon density and the carrier density decay quickly before the relaxation oscillation could occur. In order to resolve the discrepancy with the experimental result, we include the effect of carrier diffusion in the simulation. Due to the surface recombination and stimulated emission into the whispering-gallery modes, the carrier density at the edge of the disk is lower than that near the disk center. Hence, the carriers diffuse from the center toward the edge of the microdisk. The carrier diffusion should broaden the pulse of carrier injection $P_p(t)$ into the microdisk edge which overlaps the whispering gallery modes. For simplicity, we take into account the effect of carrier diffusion by increasing the width of the pump pulse $P_p(t)$. Figure 3 shows the calculated results when the FWHM of the pump pulse is equal to the carrier diffusion time in the microdisk, which is estimated to be 400 ps. The delay time hardly changes with the pump rate below the lasing threshold. It jumps from about 300 ps to less than 200 ps at the threshold where $P_0 = 9.8\times 10^{27}\,\mathrm{cm}^{-3}\,\mathrm{s}^{-1}$, and then decreases as P_0 increases [Fig. 3(a)]. The relaxation oscillation also appears in the time traces of the photon density above the threshold, as shown in Fig. 3(b). The regime near the threshold where the delay time increases with P_0 becomes much narrower, and the variation becomes less pronounced. Hence, this increase is not easy to observe in the experiment. Although the effect of carrier diffusion is included in such a simplified way in our model, the simulation results reproduce the experimental observation quite well. This agreement demonstrates that the turn-on time of the microdisk laser is determined by the carrier diffusion time. With an increase of temperature, the microdisk laser will be slowed down further as a result of the increased carrier diffusion time. As discussed above, carrier diffusion is induced partially by the surface recombination at the edge of the microdisk. In fact, the surface recombination not only leads to carrier diffusion but also reduces the lasing gain. For GaAs/AlGaAs microdisk lasers, the problem of surface recombination becomes more severe with increasing the temperature. A GaAs QW microdisk laser will not lase at 80 K unless the disk surface is passivated.[6] In order to increase the efficiency and the speed of a microdisk laser, the surface recombination should be suppressed. One way to eliminate surface recombination is to replace the quantum wells with the quantum dots inside the microdisk.[11]

In summary, we have investigated experimentally the dynamic response of a GaAs/AlGaAs microdisk laser under femtosecond optical pumping. Below the lasing threshold, the delay time of the emission pulse from the microdisk hardly changes with the pump power. However, above the lasing threshold, the delay time is shortened dramatically, and it decreases with the increase of the pump power. The theoretical simulation based on the rate equations reproduce the experimental observation after the effect of carrier diffusion is taken into account. The simulation result illustrates that the speed of a microdisk laser is limited mainly by the carrier diffusion in the disk plane.

This work is supported by the National Science Foundation under Grant No. ECS-9800068.

[1] T. Baba, IEEE J. Sel. Top. Quantum Electron. **3**, 808 (1997).
[2] S. L. McCall, A. F. J. Levi, R. E. Slusher, S. J. Pearton, and R. A. Logan, Appl. Phys. Lett. **60**, 289 (1992).
[3] A. F. J. Levi, S. L. McCall, S. J. Pearton, and R. A. Logan, Electron. Lett. **29**, 1666 (1993).
[4] R. E. Slusher, A. F. J. Levi, U. Mohideen, S. L. McCall, S. J. Pearton, and R. A. Logan, Appl. Phys. Lett. **63**, 1310 (1993).
[5] D. Y. Chu, M. K. Chin, W. G. Bi, H. Q. Hou, C. W. Tu, and S. T. Ho, Appl. Phys. Lett. **65**, 3167 (1994).
[6] U. Mohideen, W. S. Hobson, S. J. Pearton, F. Ren, and R. E. Slusher, Appl. Phys. Lett. **64**, 1911 (1994).
[7] A. F. J. Levi, R. E. Slusher, S. L. McCall, T. Tanbun-Ek, D. L. Coblentz, and S. J. Pearton, Electron. Lett. **28**, 1010 (1992).
[8] A. F. J. Levi, R. E. Slusher, S. L. McCall, S. J. Pearton, and W. S. Hobson, Appl. Phys. Lett. **62**, 2021 (1993).
[9] T. Baba, M. Fujita, A. Sakai, M. Kihara, and R. Watanabe, IEEE Photonics Technol. Lett. **9**, 878 (1997).
[10] T. Baba, IEEE J. Sel. Top. Quantum Electron. **5**, 673 (1999).
[11] H. Cao, J. Y. Xu, W. H. Xiang, Y. Ma, S.-H. Chang, S. T. Ho, and G. S. Solomon, Appl. Phys. Lett. **76**, 3519 (2000).
[12] R. E. Slusher and U. Mohideen, in *Optical Processes in Microcavities*, edited by R. K. Chang and A. J. Campilla (World Scientific, Singapore, 1996), p. 315.
[13] G. P. Agrawal, and N. K. Dutta, *Semiconductor Lasers* (Van Nostrand Reinhold, New York, 1993), Chap. 6.
[14] F. Janke, H. C. Schneider, and S. W. Koch, Appl. Phys. Lett. **69**, 1185 (1996).